SOIL Discuss., doi:10.5194/soil-2016-63, 2016
Manuscript under review for journal SOIL
Published: 18 October 2016

A probabilistic approach to quantifying soil property change through time integration of energy and mass input

Christopher Shepard[1*], Marcel G Schaap[1], Jon D Pelletier[2], Craig Rasmussen[1]

[1]Department of Soil, Water and Environmental Science, The University of Arizona, Tucson, AZ, USA, 85721-0038
[2]Department of Geosciences, The University of Arizona, Tucson, AZ, USA 85721-0077

*_Correspondence to_: Christopher Shepard, 1177 E Fourth St, Room 429, Shantz Building, The University of Arizona, Tucson, AZ, 85721-0038

SOIL Discuss., doi:10.5194/soil-2016-63, 2016
Manuscript under review for journal SOIL
Published: 18 October 2016

Abstract

Soils form as the result of a complex suite of biogeochemical and physical processes; however, effective modeling of soil property change and variability is still limited, and does not yield widely applicable results. We suggest that predicting a distribution of probable values based upon the soil-forming state factors is more effective and applicable than predicting discrete values. Here we present a probabilistic approach for quantifying soil property variability through integrating energy and mass inputs over time. We analyzed changes in the distributions of soil texture and solum thickness as a function of increasing time and pedogenic energy (effective energy and mass transfer, EEMT) using soil chronosequence data compiled from literature. Bivariate normal probability distributions of soil properties were parameterized using the chronosequence data; from the bivariate distributions, conditional univariate distributions based on the age and flux of matter and energy into the soil were calculated, and probable ranges of each soil property determined. We tested the ability of this approach to predict the soil properties of the original soil chronosequence database, and soil properties in complex terrain at several Critical Zone Observatories in the U.S. The presented probabilistic framework has the potential to greatly inform our understanding of soil evolution over geologic time-scales. Considering soils probabilistically captures soil variability across multiple scales and explicitly quantifies uncertainty in soil property change with time.

SOIL Discuss., doi:10.5194/soil-2016-63, 2016
Manuscript under review for journal SOIL
Published: 18 October 2016

1. Introduction

The need for pedogenic models that can be widely applied and easily utilized is paramount for understanding soil-landscape evolution, soil property change with time, and predicting future soil conditions. A mathematically simple, easily parameterized approach has yet to be developed that is capable of predicting current soil properties or recreating potential soil evolution with time. Here we address this knowledge gap through development of a probabilistic model of soil property change capable of predicting soil properties across a wide range of terrains, climates, and ecosystems.

The state factor approach has been one of the primary pedogenic models since it's development in the late 1800's and early 1900's (Dokuchaev, 1883; Jenny, 1941). The soil state factor approach (Jenny, 1941) assumes the state of the soil system or specific soil properties (S) may be described as a function of the external environment, represented by climate (cl), biology (o), relief (r), parent material (p), and time (t): S = f(cl, o, r, p, t). This approach increased our understanding of soil variation across each factor, but more complex, multivariate approaches are generally not possible or difficult to derive from this formulation (Yaalon, 1975). From the original state factor model have evolved pedogenic models that include functional approaches (Jenny, 1961), energetic approaches (Rasmussen and Tabor, 2007; Rasmussen et al., 2005, 2011; Runge, 1973; Smeck et al., 1983; Volobuyev, 1964), and mechanistic approaches (Finke, 2012; Minasny and McBratney, 1999; Salvador-Blanes et al., 2007; Vanwalleghem et al., 2013). However, many of these approaches are either limited to a site-specific basis, require a high degree of parameterization, or lack wide-scale applicability.

Here we develop a simple probabilistic approach to predict soil physical properties using a large dataset of chronosequences studies. The model compresses state factor variability into 2

SOIL Discuss., doi:10.5194/soil-2016-63, 2016
Manuscript under review for journal SOIL
Published: 18 October 2016

77 key components (parent material and total pedogenic energy, defined in Section 1.1) that were
78 parameterized and calibrated using the chronosequence database. Additionally, we modified the
79 model to include soil depth to capture the influence of redistributive hillslope processes to
80 predict soil properties. We hypothesized that by including soil depth, the model would
81 effectively predict the clay content in an independent dataset synthesizing soil and landscape
82 variability in complex, hilly terrain from a wide range of environments.
83
84 **1.1 Probabilistic model of soil property change**
85 The model presented here is based on a reformulated state-factor model, where a location
86 has a probability of displaying a range of differing soil morphologies and properties based upon
87 the state factors, with some range of values more probable than others, meaning the state-factor
88 model (Jenny, 1941) may be restated as:

89 $$\mathbb{P}(s_1 \leq S \leq s_2) = f(cl, o, r, p, t) \qquad (1)$$

90 where, the left hand side of the equation, $\mathbb{P}(s_1 \leq S \leq s_2)$, represents the probability that a given
91 soil will have a value located between a lower limit (s_1) and an upper limit (s_2) (Phillips, 1993b).
92 Eq. 1 can be restated more simply as:

93 $$\mathbb{P}(s_1 \leq S \leq s_2) = f(L_o, P_x, t) \qquad (2)$$

94 where, the original soil forming state factors have been simplified to represent the fluxes of
95 matter and energy into the soil system (P_x), incorporating the influence of climate and biology,
96 and the initial state of the soil forming conditions (L_o), incorporating the influence of the initial
97 topography and original soil parent material, and time or age of the soil system (t) (Jenny, 1961).
98 Equation 2 was further simplified to make the approach operational. A quantitative
99 measure of climate and biology was needed to represent the influence of P_x on soil formation.

SOIL Discuss., doi:10.5194/soil-2016-63, 2016
Manuscript under review for journal SOIL
Published: 18 October 2016

100 We used a quantification of P_x calculated from effective precipitation and biological
101 productivity, termed effective energy and mass transfer (EEMT, J m^{-2} yr^{-1})(Rasmussen and
102 Tabor, 2007; Rasmussen et al., 2005, 2011). EEMT provides a measure of the energy transferred
103 to the subsurface, in the form of reduced carbon from primary productivity and heat transfer
104 from effective precipitation, which has the potential to perform pedogenic work, e.g., chemical
105 weathering and carbon cycling. Using EEMT as a simplification of P_x, Eq. 2 was restated as
106 (Rasmussen et al., 2011):

107 $$\mathbb{P}(s_1 \leq S \leq s_2) = f(L_o, EEMT, t) \qquad (3)$$

108 We further simplified Eq. 3 by combining the flux term EEMT and the age of the soil system (t).
109 EEMT multiplied by the age of the soil system, i.e. EEMT*t, provides an estimate of the total
110 energy transferred to the soil system over the course of its evolution, referred to here as "total
111 pedogenic energy" (TPE, J m^{-2}). The TPE provides an estimate of P_x that incorporates soil age,
112 thus Eq. 3 may be restated as:

113 $$\mathbb{P}(s_1 \leq S \leq s_2) = f(L_o, TPE) \qquad (4)$$

114 where at a certain point in time the probability of a soil property existing between s_1 and s_2 is a
115 function of L_o and TPE. Explicitly including time in Eq. 4 through TPE partially captures
116 variation in soil property change attributable to topography and parent material. Soil residence
117 time may be directly related to landscape position through topographic control on soil production
118 and sediment transport/deposition (Heimsath et al., 1997, 2002; Yoo et al., 2007). Additionally,
119 parent material modulates soil residence time through control on soil depth (Heckman and
120 Rasmussen, 2011; Rasmussen et al., 2005), soil production, and sediment transport rates (Andre
121 and Anderson, 1961; Portenga and Bierman, 2011). The initial conditions of the soil forming
122 system (L_o) are never fully known; however, representing the state of the soil system as a

SOIL Discuss., doi:10.5194/soil-2016-63, 2016
Manuscript under review for journal SOIL
Published: 18 October 2016

123 probable distribution of values, implicitly accounting for soil age, and not constraining the initial
124 soil forming conditions, Eq. 4 can be stated simply as:

125 $$\mathbb{P}(s_1 \leq S \leq s_2) = f(TPE) \qquad (5)$$

126 where the probability state of the soil, $\mathbb{P}(s_1 \leq S \leq s_2)$, bounded by a lower and upper limit, is a
127 function of one quantifiable variable.

128 Quantitatively realizing Eq. 5 required the use of predetermined joint probability density
129 functions parameterized with TPE and a selected soil physical property. Bivariate normal density
130 functions were calculated to determine the probability of a soil property range given a TPE
131 value. The bivariate normal density distribution (Ugarte et al., 2008) was calculated as:

132 $$f(x,y) = \frac{1}{2\pi\sigma_x\sigma_y\sqrt{1-\rho^2}} \exp\left(-\frac{1}{2(1-\rho^2)}\left[\frac{(x-\mu_x)^2}{\sigma_x^2} + \frac{(y-\mu_y)^2}{\sigma_y^2} - \frac{2\rho(x-\mu_x)(y-\mu_y)}{\sigma_x\sigma_y}\right]\right) \qquad (6)$$

133 where, ρ represents the correlation coefficient, μ_x is the mean of TPE, μ_y is the mean of the
134 selected soil physical property, σ_x is the standard deviation of TPE, σ_y is the standard deviation
135 of the selected soil physical property. Using the bivariate normal density functions, conditional
136 mean and variance values were calculated given a value of TPE; the conditional means and
137 variances parameterized conditional univariate normal distributions for the selected soil physical
138 properties. The conditional mean (Ugarte et al., 2008) was calculated as:

139 $$\mu_{Y|X=x} = \mu_y + \rho\frac{\sigma_y}{\sigma_x}(x - \mu_x) \qquad (7)$$

140 where, $\mu_{Y|X=x}$ is the conditional mean soil property value given a value for TPE. The conditional
141 variance (Ugarte et al., 2008) was calculated as:

142 $$\sigma^2_{Y|X=x} = \sigma_y^2(1 - \rho^2) \qquad (8)$$

143 where, $\sigma^2_{Y|X=x}$ is the conditional variance of the soil property given a value of TPE.

SOIL Discuss., doi:10.5194/soil-2016-63, 2016
Manuscript under review for journal SOIL
Published: 18 October 2016

144 Applying this approach required certain assumptions and simplifications. The model
145 assumes that climate was constant over the entire duration of pedogenesis. The model makes no
146 assumptions about the progressive and regressive processes that drive pedogenesis; by weighing
147 all profiles equally, both progressive (e.g., horizonation, clay accumulation, reddening, etc.) and
148 regressive (e.g., haplodization, erosion, pedoturbation, etc.) pedogenic processes (Johnson and
149 Watson-Stegner, 1987; Phillips, 1993a), are implicitly captured in the model structure. The
150 model makes no assumptions about the initial soil forming system; the model simply describes
151 the probability of a location exhibiting a range of soil properties based on TPE. The model
152 assumes all changes in soil physical properties are due to pedogenic processes. We used a
153 bivariate normal distribution; consequently the model assumes the data conforms to a normal
154 distribution.
155
156 **2. Methods**
157 **2.1 Data collection and preparation**
158 The probability distributions were parameterized using an extensive literature review of
159 chronosequence studies. Over 140 chronosequence publications were identified using Google
160 Scholar (scholar.google.com) and ThomsonReuters Web of Science (webofknowledge.com),
161 forty-five of which contained the data required for inclusion within the present study. Inclusion
162 within the present study required: profile descriptions with horizon-level clay, sand, and silt
163 content, soil depth; well-defined ages of the soil-geomorphic surfaces; and geographic
164 coordinates or maps showing locations of the described profiles. The chronosequences spanned a
165 wide range of geographic locations, ecosystems, climates, rock types, and geomorphic landforms
166 (Fig 1, Table S1).

SOIL Discuss., doi:10.5194/soil-2016-63, 2016
Manuscript under review for journal SOIL
Published: 18 October 2016

167

168 **2.2 Total Pedogenic Energy**

169 The influence of both climate and vegetation at the locations of each soil profile was
170 determined using effective energy and mass transfer (EEMT) (Rasmussen and Tabor, 2007;
171 Rasmussen et al., 2005). The EEMT values for each soil profile were extracted from a global
172 map of EEMT derived from the monthly global climate dataset of New et al. (1999) at 0.5°x0.5°
173 resolution using ArcMap 10.1 (ESRI, Redlands, CA) (Rasmussen et al., 2011). Total pedogenic
174 energy (TPE, J m^{-2}) was derived simply by multiplying EEMT (J m^{-2} yr^{-1}) for each soil profile by
175 its reported age (yr). TPE was used because it was a better predictor of soil physical properties
176 relative to mean annual temperature, mean annual precipitation, or net primary productivity
177 (Table 3).

178

179 **2.3 Application to chronosequence data**

180 The chronosequence database included 45 distinct chronosequences representing 416
181 different soil profiles. We focused here on changes in sand, silt, and clay content and solum
182 thickness as proxies for soil change with time. We tested the approach on depth weighted (DWT)
183 sand, silt and clay content (reported as weight %), as well as the maximum measured value of
184 sand, silt, and clay content within each soil profile. Buried horizons were removed from the soil
185 profiles before either the maximum or DWT content values were calculated. For soils reported in
186 McFadden et al. (1986), surficial modern-aged eolian horizons were removed; the reported ages
187 of the soil-geomorphic surface more closely matched the buried horizons under the eolian
188 horizons. Solum thickness was extracted for each profile, defined as the thickness of the horizons
189 influenced by pedogenic processes or the depth to C horizons (Schaetzl and Anderson, 2005).

SOIL Discuss., doi:10.5194/soil-2016-63, 2016
Manuscript under review for journal SOIL
Published: 18 October 2016

190 The site RW-14 from McFadden and Weldon (1987) was not included in the solum thickness
191 model calculations, the measured solum thickness of RW-14 was 1460 cm, an order of
192 magnitude greater than all other soil profiles included in the study. Four hundred and sixteen
193 profiles reported clay content data, only 398 profiles reported sand and silt content, and 410 soil
194 profiles contained a developed solum. We classified the soil profiles by parent material in terms
195 of igneous, metamorphic, or sedimentary and by geomorphic landform (e.g., alluvial surface,
196 marine terrace, or moraine, etc.) (Shoeneberger et al., 2012); for example, if a soil was formed on
197 an alluvial fan from granitic parent material, it would be defined as alluvial and igneous.

198 Using the soils data, we calculated bivariate normal probability distributions using TPE
199 and the soil physical properties (Eq. 6). The soil data were transformed using logarithmic and
200 square root transformations when appropriate to meet the normality assumption of the bivariate
201 normal probability distribution. Conditional univariate normal distributions (Eqs. 7, 8) were
202 calculated to approximate probable ranges of soil properties using leave one out cross validation
203 (LOOCV). Each of the soil chronosequences was removed from the model dataset, with the
204 remaining chronosequence data used to calculate the parameters of the bivariate and conditional
205 univariate normal distributions. The conditional univariate normal distributions were calculated
206 using the TPE values for the profiles within the left-out chronosequence.

207

208 **2.4 Application to complex terrain**

209 By design, soil chronosequences are generally sited on gentle, low sloping terrain to
210 minimize the influence of topography and erosion/deposition on soil formation (Harden, 1982).
211 However, much of the Earth's surface is characterized by complex topography with high relief,
212 steep slopes, and differences in slope aspect. Any predictive soil model or approach must be

SOIL Discuss., doi:10.5194/soil-2016-63, 2016
Manuscript under review for journal SOIL
Published: 18 October 2016

effective in both simple terrain and complex terrain. To test the ability of the model to predict soil properties in complex terrain, we compiled data from upland catchments with variable parent material and topography from the literature, as well as data available from the US NSF Critical Zone Observatory Network (CZO, wwww.criticalzone.org) (Table 1) (Bacon et al., 2012; Dethier et al., 2012; Foster et al., 2015; Holleran et al., 2015; Lybrand and Rasmussen, 2015; Rasmussen, 2008; West et al., 2013). Data from several additional studies from complex terrain were also included to test the model (Table 1) (Dixon et al., 2009; Yoo et al., 2007). These data were accessed from: www.criticalzone.org, or Google Scholar (scholar.google.com). These studies were included because they all contained horizon-level soil texture data, soil depth, percent volume rock fragment data, and ^{10}Be or U-series measures of soil erosion rates or residence time, where mean residence time (MRT) was calculated as: MRT=h/E, where h is soil depth (m) and E is erosion rate (m/yr) (Pelletier and Rasmussen, 2009b). We used published coordinates to extract EEMT values, calculated from New et al. (1999), for each soil profile using ArcGIS 10.1, and used EEMT and MRT to calculate TPE. It should be noted the coarse resolution of New et al. (1999) EEMT values do not account for local scale variation in water redistribution and primary productivity that can lead to significant topographic variation in EEMT (Rasmussen et al., 2015). Using Eq. 6 and the parameters generated from the chronosequence database, conditional mean depth weighted clay content was calculated for each profile.

Due to the influence of redistributive hillslope processes on soil development (Yoo et al., 2007), soil depth varies systematically across hillslopes (Heimsath et al., 1997); thus, soil depth can be used to incorporate information about these processes within the model calculations. We

SOIL Discuss., doi:10.5194/soil-2016-63, 2016
Manuscript under review for journal SOIL
Published: 18 October 2016

235 calculated the mass per area clay content of these profiles using soil depth to correct for these
236 processes, as:

237 $$\text{Mass per area clay (kg m}^{-2}) = (\rho_b)(h)\left(\frac{\mu_{Y|X=x,\text{DWT CLAY}}}{100}\right)\left(1-\left(\frac{\text{RF\%}}{100}\right)\right) \quad (9)$$

238 where, ρ_b is the soil bulk density assumed to be 1500 kg m^{-3} for all soil profiles, $\mu_{Y|X=x,\text{ DWT CLAY}}$
239 is the predicted conditional mean for depth weighted clay content (DWT CLAY) using Eq. 7,
240 RF% is the measured depth weighted percent volume rock fragments within the soil, when no
241 RF% data were available we assumed a value of 41.7%, which was the average RF% for profiles
242 with reported values, and h is the soil depth in meters. Using Eq. 9, mass per area clay was
243 calculated for each soil profile. Further, we examined the impact of depth, rock fragment
244 percentage, and predicted conditional mean DWT clay on the predicted mass per area clay
245 predictions using multiple linear regression.
246
247 **2.4.1 Coupling geomorphic model with probabilistic model**
248 Additionally, we applied the model independent of measured soil data, across a small
249 complex catchment in the Santa Catalina Mountains (Catalina-Jemez CZO, Fig 2a-b, Table 1)
250 (Holleran et al., 2015; Lybrand and Rasmussen, 2015). The ~6 ha catchment is located at an
251 elevation between 2300-2500 m with mixed conifer vegetation, approximately 30 km northeast
252 of Tucson, AZ (Fig 2, Table 1). The approach utilized soil depth and residence time output from
253 a process-based numerical soil depth model. The model used high resolution LiDAR derived
254 topographic data to estimate 2 m pixel resolution soil depth and erosion rates (Fig 2c) (Pelletier
255 and Rasmussen, 2009a). These data were coupled with topographically resolved EEMT values
256 that accounted for local hillslope scale variation in water redistribution and primary productivity
257 at a 10 m pixel resolution (Rasmussen et al., 2015) (Fig 2d). We used TPE based on modeled

SOIL Discuss., doi:10.5194/soil-2016-63, 2016
Manuscript under review for journal SOIL
Published: 18 October 2016

258 EEMT and soil residence time to predict DWT clay, and coupled with modeled depth in Eq. 9 to
259 predict mass per area clay at 2 m pixel resolution. We assumed a constant 50% rock fragment
260 value for each location. The coupled geomorphic-TPE model outputs were compared with point
261 measures of mass per area clay from Holleran et al. (2015) and Lybrand and Rasmussen (2015).
262 Model data were completely independent from Holleran et al. and Lybrand and Rasmussen and
263 these datasets served as a validation for the modeled output.
264
265 **3. Results**
266 **3.1 Application and parameterization to chronosequences**
267 The relationships between TPE and soil texture and solum thickness were used to
268 calculate the bivariate probability distributions. The bivariate probability distributions (Eq. 6)
269 were parameterized using the chronosequence database (Table 2). Furthermore, the relationship
270 between TPE and the soil properties was stronger than just using age, NPP, MAP, or MAT alone
271 (Table 3). Age was expected to strongly correlate to the soil properties due to the design of
272 chronosequence studies; however, comparing age and TPE separately, the percent increase in
273 Spearman rank correlations (r) ranged from 1.9% (DWT Silt) to 22.4% (Max Sand). Maximum
274 and depth weighted silt content were weakly correlated to both age and TPE and exhibited only a
275 minimal change in Spearman's rank correlation with TPE relative to age.
276 The correlation between TPE and maximum clay content (Fig 3, ρ=0.78, r^2=0.61,
277 $\sqrt{\text{Max Clay}} = -7.35 + 1.36 * \log(\text{TPE})$, df=414) was highly significant, and presented the
278 strongest probabilistic relationship determined between TPE and the soil properties. The
279 bivariate probability surface displayed the greatest probability around the joint means between
280 TPE and maximum clay content (Fig 3). Solum thickness and TPE were also strongly related,

SOIL Discuss., doi:10.5194/soil-2016-63, 2016
Manuscript under review for journal SOIL
Published: 18 October 2016

281 but weaker relative to the maximum clay-TPE relationship (Fig S1, ρ=0.65, r^2=0.42,
282 $\log(\text{solum thickness}) = -0.57 + 0.27 * \log(\text{TPE})$, df=408). The relationships between TPE
283 and max sand (Fig S2) and silt (Fig S3) contents were generally weaker, relative to clay and
284 solum thickness, with little to no relationship between TPE and silt content.

285 The conditional univariate normal distribution parameters were determined for the soil
286 physical properties from the bivariate distribution and using Eqs. 7 and 8. The bivariate normal
287 distribution effectively predicted maximum clay content (Fig 4) with an r^2 = 0.54
288 (RMSE=14.7%) between the measured maximum clay content and predicted conditional mean
289 maximum clay content (Eq. 7) across all sites based on LOOCV (Fig 4d). The model effectively
290 predicted maximum clay content for each parent material with r^2 of 0.60 (RMSE=14.1%), 0.56
291 (RMSE=11.9%), and 0.59 (RMSE=16.7%), for igneous, metamorphic, and sedimentary parent
292 materials, respectively. The r^2 between the measured values and predicted values for solum
293 thickness, max sand, and max silt were 0.28 (RMSE=99.8 cm, Fig S4), 0.17 (RMSE=23.2%, Fig
294 S5), and 0.04 (RMSE=18.0%, Fig S6), respectively.

295 The relationship of predicted to actual maximum clay content varied significantly across
296 individual studies. The predicted values represent the predicted conditional means (Eq. 7)
297 bounded by the conditional standard deviation (Eq. 8), which approximates a 50% probability
298 that the measured maximum clay content will be within 1 standard deviation of the conditional
299 mean (Fig 5). The individual studies presented in Fig 5 were selected to represent a broad range
300 of climates and landforms, and demonstrate both the strengths and weaknesses of the model. For
301 Harden (1987) (Fig 5a, r^2=0.88, $p<0.0001$, df=20, RMSE=9.3%) and Howard et al. (1993) (Fig
302 5b, r^2=0.86, $p<0.001$, df=6, RMSE=9.8%), the model was generally successful at predicting the
303 maximum clay content values; both the Harden (1987) and Howard et al. (1993) sequences were

SOIL Discuss., doi:10.5194/soil-2016-63, 2016
Manuscript under review for journal SOIL
Published: 18 October 2016

304 located in alluvial deposits but in vastly different climates, xeric (winter-dominated annual
305 rainfall regime) vs. udic (evenly distributed annual rainfall regime), respectively. The model was
306 capable of predicting maximum clay content values for glacial moraine deposits, in a frigid
307 climate (Fig 5c, r^2=0.87, p<0.0001, df=12, RMSE=6.1% Birkeland, 1984) and on marine terraces
308 in Northern California with a xeric climate (Fig 5f, r^2=0.98, p<0.001, df=4, RMSE=8.7%,
309 Merritts et al., 1991). The model was incapable of predicting clay accumulation on marine
310 terraces in hot, wet climates in Barbados (Fig 5d, r^2=0.31, p=0.08, df=9, RMSE=45.1% Muhs,
311 2001) or Taiwan (Fig 5e, r^2=0.67, p<0.001, df=11, RMSE=23.2%, Huang et al., 2010).
312
313 **3.2 Application in complex terrain**
314 The model was much less effective in complex terrain and highly overpredicted DWT
315 clay contents in soils located in complex landscapes (Fig 6a, r^2=0.26, y=0.39x+7.27, p<0.0001,
316 RMSE=5.3%). The model highly over predicted the clay content of the South Carolina site and
317 the Gordon Gulch soils, and under predicted the clay content of the Rincon, Santa Catalina,
318 Jemez sites.
319 When correcting for the influence of hillslope processes by explicitly including soil depth
320 and calculating mass per area clay, the approach effectively predicted clay content, with an
321 r^2=0.81 (Fig 6b, y=1.56x-15.2, p<0.0001, RMSE=84.4 kg clay m^{-2}), only slightly overpredicting
322 clay content, with a slope of 1.56. Soil depth was the strongest contributing factor to the mass per
323 area clay prediction with the greatest sums of squares in a simple multiple linear regression
324 including depth, RF%, and DWT clay% (Table 4); predicted conditional mean clay content
325 percentage was the second strongest contributing factor to the mass per area clay prediction.
326 Rock fragment percentage did not influence the mass per area clay content prediction.

SOIL Discuss., doi:10.5194/soil-2016-63, 2016
Manuscript under review for journal SOIL
Published: 18 October 2016

327

328 **3.3 Coupled geomorphic-TPE model**

329 The coupled geomorphic-TPE model effectively predicted mass per area clay for the
330 majority of soils located within the Marshall Gulch subcatchment with an r^2=0.74 (Fig 7a,
331 y=0.85x-5.00, p<0.0001, RMSE=17.7 kg clay m^{-2}). For a subset of soils, the model did not
332 effectively predict mass per area clay, and were excluded from the regression in Fig 7a; four of
333 these soils were located on the east-facing ridge of the catchment, and an additional two soils
334 were formed on amphibolite rather than the granite or quartzite materials that all of the other
335 soils in the catchment were derived from. All of these locations also exhibited a poor fit between
336 modeled and measured soil depth (Fig 2e). The spatial distribution of mass per area clay was also
337 predicted across the catchment (Fig 7b), independently of measured data, and generally
338 conformed to previously predicted spatial distribution of clay stocks in the Marshall Gulch
339 catchment (Holleran et al., 2015).

340

341 **4. Discussion**

342 **4.1 Model effectiveness**

343 **4.1.1 Model results for chronosequences**

344 The model predicted maximum clay content across a diverse range of lithologies,
345 climates, and landforms. Weathering and clay production are primary pedogenic processes
346 (Birkeland, 1999; Schaetzl and Anderson, 2005), and because the model assumed all changes in
347 the soil profile are due to these processes, the model was the most effective at predicting clay
348 content. For initial soil states that begin pedogenesis with a potentially significant amount of
349 clay-sized particles the model was much less effective. The soils of the Taiwanese

SOIL Discuss., doi:10.5194/soil-2016-63, 2016
Manuscript under review for journal SOIL
Published: 18 October 2016

chronosequence formed from conglomerates (Huang et al., 2010); conglomerates are typically poorly sorted, such that these soils initially formed with high clay contents slowing clay accumulation, limiting the effectiveness of the model to predict clay contents in these soils. Additionally, the model highly underestimated the clay content of soils located on coral reef terraces in tropical environments (Maejima et al., 2005; Muhs, 2001). Coral reef terraces represent a relatively unique landform that weathers rapidly to fine sized particles, especially under tropical climates, and generally have complicated parent material compositions (Muhs et al., 1987). The combination of these factors limited the ability of the model to predict the soil properties on these surfaces.

Sand and silt displayed weaker relationships with increasing total pedogenic energy. The lack of correlation of sand and silt to TPE may result in part from the definitions of the particle size classes. Sand sized particles span several orders of magnitude difference in particle size, ranging from particles of 2 mm to 0.05 mm (Soil Survery Staff, 2010), whereas clays are constrained to particles less than 0.002 mm. The sequential weathering of rock fragments and coarse sand to fine and very fine sands therefore is not reflected in total sand content and likely diminishes the relationship between sand content and total pedogenic energy and time (Pye and Sperling, 1983; Pye, 1983; Sharmeen and Willgoose, 2006). The relationship between silt content and pedogenic energy was the weakest of the three broad particles size classes (Tables 2, 3). Similar to sand, the silt size fractions span an order of magnitude in particle size ranging from 0.05 to 0.002 mm in diameter. Additionally, the silt fraction may also be heavily influenced by deposition of eolian material and thereby introduce an additional mass of silt that was not derived from the direct weathering of the initial soil forming system (McFadden et al., 1987) effectively uncoupling silt content from total pedogenic energy.

SOIL Discuss., doi:10.5194/soil-2016-63, 2016
Manuscript under review for journal SOIL
Published: 18 October 2016

373 Solum thickness displayed a relatively strong relationship with increasing pedogenic
374 energy, with TPE explaining up to 42% of the variance in solum thickness (Tables 2, 3). Soil
375 production is related to climatic variation (Amundson et al., 2015), with this variation partly
376 captured by EEMT and TPE, leading to the slightly stronger predictive power of the model.
377 However, soil production is also highly influenced by redistributive hillslope process, chemical
378 and physical weathering, and tectonic uplift (Heimsath et al., 1997; Riebe et al., 2004; Yoo and
379 Mudd, 2008b), and can be a highly non-linear process (Pelletier and Rasmussen, 2009a). These
380 factors were not directly accounted for in this study in that topography was not a quantified
381 factor, which likely represents a large proportion of the remaining unexplained variance in solum
382 thickness.
383
384 **4.1.2 Model results in complex terrain**
385 Due to using soil chronosequence data to parameterize the approach, the influence of
386 redistributive hillslope processes was not captured. Additionally, in the amount of time required
387 to transport soil across a hillslope, chemical and physical alterations of the soil particles are
388 possible and may not be reflected in mean residence time calculations (Yoo and Mudd, 2008a;
389 Yoo et al., 2007). Soil thickness is highly dependent upon hillslope position and landscape
390 morphology (Dietrich et al., 2003; Heimsath et al., 1997; Pelletier and Rasmussen, 2009a). By
391 using soil thickness as a proxy for the strength of these redistributive hillslope processes, and
392 converting the predicted conditional mean clay content value to a mass per area basis, the model
393 was able to capture differences in clay content across complex terrain for a variety of lithologies
394 and climates. The differing lithologies, climates, or vegetation types did not appear to impact the
395 ability of the model to predict clay contents, likely because soil depth accounts for many of these

SOIL Discuss., doi:10.5194/soil-2016-63, 2016
Manuscript under review for journal SOIL
Published: 18 October 2016

396 controls. Parent material and climate influence the weathering process and production of clay in
397 soils (Harden and Taylor, 1983; Muhs et al., 2001); however, these factors are collinear with soil
398 depth (Heckman and Rasmussen, 2011; Lybrand and Rasmussen, 2015; Pelletier and Rasmussen,
399 2009a), such that by including soil depth, differences due to lithology or climate were partly
400 incorporated in the model prediction.
401
402 **4.1.3 Results from coupled geomorphic-TPE model**
403 For the majority of sites in the Marshall Gulch sub-catchment, the coupled geomorphic-
404 TPE model was highly effective at predicting clay content, and the spatial distribution of clay
405 stocks. Large differences were found for four soils located on the east-facing ridge of the
406 catchment underlain by granite with the model generally over-predicting soil depth and clay
407 content. Discrepancies between the modeled and measured depths were likely the primary
408 sources of error within the mass per area clay predictions for the 4 east-facing ridge soils (Fig
409 2e). The geomorphic model predicted deeper soil depths due to the presence of an apparent
410 convergent zone on the east-facing ridge of the sub-catchment; however, this convergent zone is
411 only a small feeder tributary to the larger catchment drainage. The inability of the model to
412 effectively predict clay contents and the mismatch between modeled and actual soil depths in the
413 4 soils located on the east-facing ridge is likely due to this local, fine-scale topographic variation
414 Error in predicted soil depths due to fine-scale differences in lithology within the
415 Marshall Gulch sub-catchment partly explains the discrepancies between measured and predicted
416 mass per area clay contents. For two amphibolite-derived soils, the model greatly underestimated
417 mass per area clay. The geomorphic soil depth model assumed a uniform weathering rate based
418 on the granitic soils (Pelletier and Rasmussen, 2009a); due to differences in primary mineral

SOIL Discuss., doi:10.5194/soil-2016-63, 2016
Manuscript under review for journal SOIL
Published: 18 October 2016

419 assemblage, the amphibolite materials are likely weather at a faster rate compared to the granite
420 derived soils (White et al., 2001; Wilson, 2004), resulting in greater clay production and likely
421 explaining the underestimated clay contents. Inclusion of differential weathering rates for
422 varying lithologies within the geomorphic model would likely lead to better prediction of clay
423 contents. With these adjustments, the coupled geomorphic-TPE model represents an effective,
424 independent prediction of clay stocks.
425
426 **4.2 Advantages of probabilistic approach**
427 Simplifying and representing the soil-forming factors as multivariate distributions and
428 probabilities has the potential to quantitatively represent the general state-factor model, making
429 the approach universally applicable. The initial state of the soil can likely never be fully known,
430 leading to variability in soil properties over time that cannot necessarily, or ever, be attributed to
431 any external factor (Phillips, 1989, 1993b). A probabilistic approach utilizes that variability to
432 drive predictions and understanding of these systems. Similar to the approach taken here,
433 building distributions of the soil-forming state factors that are associated with distributions of
434 particular soil properties could yield probabilistic predictions of soil formation and change. We
435 selected to use a representation of climate and biology (EEMT), however, depending on the soil
436 property of interest the variables needed to parameterize the distributions would likely change;
437 for example, if interested in organic matter content, aboveground net primary productivity or
438 normalized difference vegetation index may be better predictors of organic matter accumulation.
439 The strength of this approach lies in the fact that no assumptions are made about the initial
440 conditions of the soil forming system or the specific soil forming processes. Predicting probable
441 distributions of soil physical properties implicitly acknowledges that our understanding of any

SOIL Discuss., doi:10.5194/soil-2016-63, 2016
Manuscript under review for journal SOIL
Published: 18 October 2016

system is incomplete, but explicitly quantifies uncertainty in predictions and constrains the potential observable values to a predicted range. Utilizing this approach will require the necessary data to build distributions that are widely representative and applicable to most locations (Yaalon, 1975). With wide accessibility to large databases of soil information, such as the US National Soil Information System (NASIS) and the FAO Harmonized World Soil Database, access to the required amount and quality of data may be possible. Similar to the present study, simple bivariate distributions could be solved to calculate conditional distributions based on the soil-forming state factors, effectively producing quantitative probabilistic representations of Jenny's original equation (Jenny, 1941).

The simplicity of the present approach allows easy integration into pre-existing geomorphic models of landscape evolution. Past approaches that have combined pedogenic and landscape evolution models have generally focused on producing hypothetical soil-landscape relationships that progress forward through time (Minasny and McBratney, 2001; Vanwalleghem et al., 2013), or have focused on idealized landscapes (Temme and Vanwalleghem, 2015). However, by combining probabilistic approaches parameterized using known landscapes, and geomorphically based landscape evolution models, both potential soil-landscape evolution scenarios can be investigated, as well as predictions of the current state of the soil-landscape. As was demonstrated in Fig 7B, combining the present approach with geomorphically based soil depth models generated from DEMs has great potential to predict soil properties across a diverse range of environments, without needing prior knowledge of the landscape other than topography and climate.

4.3 Limitations and potential refinements

SOIL Discuss., doi:10.5194/soil-2016-63, 2016
Manuscript under review for journal SOIL
Published: 18 October 2016

There are obvious limitations within the current model: lack of consideration of parent material influences, topographic variation, or internal soil feedbacks and thresholds, and differences in paleoclimate variation. Parent material control on the relative proportion of weatherable minerals and mineral weathering rates (Jackson et al., 1948) can manifest as vastly different soil morphologies and rates of pedogenesis when controlling for other soil forming factors (Heckman and Rasmussen, 2011; Parsons and Herriman, 1975). The current approach implicitly assumes no information about the initial conditions, only that all clay production is a pedogenic process. Applying this approach to parent materials, where a large fraction of clay-sized particles formed through non-pedogenic processes, is thus limited and may explain why the model was ineffective for some soils. Refining the current approach would require normalization of soil to the particle size distribution of the soil parent material. Past studies have utilized highly characterized parent material data to model soil property change with time (Chadwick et al., 1990; Harden, 1982), but these data are generally difficult to obtain and often not reported in the available chronosequence literature.

Topography dictates soil chemical and physical properties and residence times, especially in complex terrain (Almond et al., 2007; Egli et al., 2008; Lybrand and Rasmussen, 2015), where non-linear diffusive hillslope processes control the fluxes of matter and energy into and out of the soil system (Heimsath et al., 1997; Pelletier and Rasmussen, 2009a; Rasmussen et al., 2015; Yoo and Mudd, 2008b; Yoo et al., 2007). Using earlier versions of EEMT (Rasmussen and Tabor, 2007; Rasmussen et al., 2005), the current formulation of the model and TPE does not explicitly quantify topographic variation, which may account for error within current soil property distributions and predictions. With the inclusion of topographic variation within EEMT (Rasmussen et al., 2015) and topographic control of soil residence times (Foster et al., 2015;

SOIL Discuss., doi:10.5194/soil-2016-63, 2016
Manuscript under review for journal SOIL
Published: 18 October 2016

488 West et al., 2013), we were able to correct this error within the present approach, particularly in
489 complex terrain, and effectively predicted clay stocks.

490 Internal or intrinsic feedbacks and thresholds within the soil system drive pedogenic
491 development without changes in the external state factors (Chadwick and Chorover, 2001; Muhs,
492 1984). For example, greater chemical weathering and clay production due to increased water
493 residence time caused by argillic horizon development is the result of an internal feedback that is
494 independent of the external climatic and biological system (Schaetzl and Anderson, 2005). These
495 thresholds can operate as progressive or regressive processes, driving soil formation forward or
496 hindering further development (Johnson and Watson-Stegner, 1987; Phillips, 1993a). Internal
497 soil development feedbacks were not explicitly considered in the present model formulation. The
498 presence of these internal feedbacks may partially explain error within the model predictions.
499 Changes in EEMT would not explain all observed differences in soil properties over the age of
500 the soil. However, if these feedbacks were operating in the included soils, the influence of
501 intrinsic thresholds was implicitly captured within the probability distributions, partially
502 accounting for the role of internal soil development feedbacks on soil formation.

503 Furthermore, global climate patterns have shifted dramatically over the last 65 Mya
504 (Zachos et al., 2001). The majority of soils observed in the compiled chronosequence database
505 span the Quaternary, including both the Holocene and Pleistocene. The Pleistocene was marked
506 by a number of major glacial-interglacial cycles at approximately 100,000-year intervals (Imbrie
507 et al., 1992; Wallace and Hobbs, 2006), which corresponded with shifting climatic conditions,
508 e.g., for large portions of the northern mid-latitudes glacial periods were generally cooler and
509 wetter, and interglacial periods were warmer and drier (Connin et al., 1998; Petit et al., 1999).
510 Further, the Pleistocene climate shifts likely influenced the rates of weathering and clay

SOIL Discuss., doi:10.5194/soil-2016-63, 2016
Manuscript under review for journal SOIL
Published: 18 October 2016

511 production (Hotchkiss et al., 2000). Taking into account the differences in past and modern
512 climate would likely diminish disparities between observed and modeled soil physical properties.
513 Reconstructed global paleo-EEMT values would improve model accuracy, and limit uncertainty
514 in the probabilistic ranges of soil properties for soils older than Holocene age.
515
516 **5. Conclusion**
517 The present approach effectively predicts soil physical properties across a diverse range
518 of geomorphic surfaces, lithologies, ecosystems, and climates. Further, this approach is
519 mathematically simple and only requires knowledge of the probable age of a geomorphic surface
520 and the effective energy and mass transfer value associated with a given location, making this
521 approach universally applicable. The simplicity of the probabilistic approach is the lack of
522 assumptions about the initial conditions of the soil forming state or the processes driving soil
523 property change. A probabilistic approach does not exactly predict a soil physical property value
524 at a given location, but constrains the probable values based upon the state of the external
525 environment to the soil. Using probabilistic approaches, we can model probable soil-landscape
526 evolution scenarios, greatly informing our understanding of the evolution of critical zone
527 structure.
528
529 **Acknowledgements**
530 We thank Molly Holleran, Rebecca Lybrand, and Ashlee Dere for providing data for this study.
531 Support for C.S. was provided by the University Fellows program at the University of Arizona.
532 This research was funded by the U.S. National Science Foundation grant no. EAR-1331408

provided in support of the Catalina-Jemez Critical Zone Observatory. LiDAR data acquisition was supported by U.S. National Science Foundation grant no. EAR-0922307 (P.I. Qinghua Guo).

References

Almond, P., Roering, J. and Hales, T. C.: Using soil residence time to delineate spatial and temporal patterns of transient landscape response, J. Geophys. Res., 112(F3), F03S17, doi:10.1029/2006JF000568, 2007.

Amundson, R., Heimsath, A., Owen, J., Yoo, K. and Dietrich, W. E.: Hillslope soils and vegetation, Geomorphology, 234, 122–132, doi:10.1016/j.geomorph.2014.12.031, 2015.

Andre, J. and Anderson, H.: Variation of Soil Erodibility with Geology, Geographic Zone, Elevation, and Vegetation Type in Northern California Wildlands, J. Geophys. Res., 66(10), 8, 1961.

Bacon, A. R., Richter, D. D., Bierman, P. R. and Rood, D. H.: Coupling meteoric 10Be with pedogenic losses of 9Be to improve soil residence time estimates on an ancient North American interfluve, Geology, 40(9), 847–850, doi:10.1130/G33449.1, 2012.

Birkeland, P. W.: Holocene soil chronofunctions, Southern Alps, New Zealand, Geoderma, 34(2), 115–134, doi:10.1016/0016-7061(84)90017-X, 1984.

Birkeland, P. W.: Soils and Geomorphology, Third., Oxford University Press, New York, New York., 1999.

Chadwick, O. A. and Chorover, J.: The chemistry of pedogenic thresholds, Geoderma, 100(3-4), 321–353, doi:10.1016/S0016-7061(01)00027-1, 2001.

Chadwick, O. A., Brimhall, G. H. and Hendricks, D. M.: From a black to a gray box — a mass balance interpretation of pedogenesis, Geomorphology, 3(3-4), 369–390, doi:10.1016/0169-555X(90)90012-F, 1990.

Connin, S., Betancourt, J. and Quade, J.: Late Pleistocene C4 plant dominance and summer rainfall in the southwestern United States from isotopic study of herbivore teeth, Quat. Res., 50, 179–193 [online] Available from: http://www.sciencedirect.com/science/article/pii/S003358949891986X (Accessed 15 February 2015), 1998.

Dethier, D. P., Birkeland, P. W. and McCarthy, J. A.: Using the accumulation of CBD-extractable iron and clay content to estimate soil age on stable surfaces and nearby slopes, Front Range, Colorado, Geomorphology, 173-174, 17–29, doi:10.1016/j.geomorph.2012.05.022, 2012.

565 Dietrich, W. E., Bellugi, D. G., Heimsath, A. M., Roering, J. J., Sklar, L. S. and Stock, J. D.:
566 Geomorphic Transport Laws for Predicting Landscape Form and Dynamics, Geophys. Monogr.,
567 135(D24), 1–30, doi:10.1029/135GM09, 2003.

568 Dixon, J. L., Heimsath, A. M. and Amundson, R.: The critical role of climate and saprolite
569 weathering in landscape evolution, Earth Surf. Process. Landforms, 34, 1507–1521,
570 doi:10.1002/esp.1836, 2009.

571 Dokuchaev, V. V.: Russian Chernozem, edited by S. Monson, Israel Program for Scientific
572 Translations Ltd. (For USDA-NSF), 1967. (Translated from Russian to English by N. Kaner).,
573 Jerusalem, Israel., 1883.

574 Egli, M., Merkli, C., Sartori, G., Mirabella, A. and Plotze, M.: Weathering, mineralogical
575 evolution and soil organic matter along a Holocene soil toposequence developed on carbonate-
576 rich materials, Geomorphology, 97(3-4), 675–696, doi:10.1016/j.geomorph.2007.09.011, 2008.

577 Finke, P. A.: Modeling the genesis of luvisols as a function of topographic position in loess
578 parent material, Quat. Int., 265, 3–17, doi:10.1016/j.quaint.2011.10.016, 2012.

579 Foster, M. A., Anderson, R. S., Wyshnytzky, C. E., Ouimet, W. B. and Dethier, D. P.: Hillslope
580 lowering rates and mobile-regolith residence times from in situ and meteoric 10 Be analysis,
581 Boulder Creek Critical Zone Observatory, Colorado, Geol. Soc. Am. Bull., 127(5-6), 862–878,
582 doi:10.1130/B31115.1, 2015.

583 Harden, J.: A quantitative index of soil development from field descriptions: Examples from a
584 chronosequence in central California, Geoderma, 28, 1–28 [online] Available from:
585 http://www.sciencedirect.com/science/article/pii/0016706182900374 (Accessed 10 March 2014),
586 1982.

587 Harden, J.: Soils Developed in Granitic Alluvium near Merced, California, USGS Bulletin 1590-
588 A, Washington, DC., 1987.

589 Harden, J. W. and Taylor, E. M.: A quantitative comparison of Soil Development in four
590 climatic regimes, Quat. Res., 20(3), 342–359, doi:10.1016/0033-5894(83)90017-0, 1983.

591 Heckman, K. and Rasmussen, C.: Lithologic controls on regolith weathering and mass flux in
592 forested ecosystems of the southwestern USA, Geoderma, 164(3-4), 99–111,
593 doi:10.1016/j.geoderma.2011.05.003, 2011.

594 Heimsath, A. M., Dietrich, W. E., Nishiizumi, K. and Finkel, R. C.: The soil production function
595 and landscape equilibrium, Nature, 388(July), 358–361, 1997.

596 Heimsath, A. M., Chappell, J., Spooner, N. A. and Questiaux, D. G.: Creeping soil, Geology,
597 30(2), 111, doi:10.1130/0091-7613(2002)030<0111:CS>2.0.CO;2, 2002.

598 Holleran, M., Levi, M. and Rasmussen, C.: Quantifying soil and critical zone variability in a
599 forested catchment through digital soil mapping, Soil, 1(1), 47–64, doi:10.5194/soil-1-47-2015,
600 2015.

601 Hotchkiss, S., Vitousek, P. M., Chadwick, O. A. and Price, J.: Climate Cycles,
602 Geomorphological Change, and the Interpretation of Soil and Ecosystem Development,
603 Ecosystems, 3(6), 522–533, doi:10.1007/s100210000046, 2000.

604 Howard, J., Amos, D. and Daniels, W.: Alluvial soil chronosequence in the Inner Coastal Plain,
605 Virginia, Quat. Res., 39, 201–213 [online] Available from:
606 http://www.sciencedirect.com/science/article/pii/S0033589483710239 (Accessed 28 May 2014),
607 1993.

608 Huang, W.-S., Tsai, H., Tsai, C.-C., Hseu, Z.-Y. and Chen, Z.-S.: Subtropical Soil
609 Chronosequence on Holocene Marine Terraces in Eastern Taiwan, Soil Sci. Soc. Am. J., 74(4),
610 1271, doi:10.2136/sssaj2009.0276, 2010.

611 Imbrie, J., Boyle, I. E. A., Clemens, S. C., Duffy, A., Howard, I. W. R., Kukla, G., Kutzbach, J.,
612 Martinson, D. G., Mclntyre, A., Mix, A. C., Molfino, B., Morley, J. J., Pisias, N. G., Prell, W. L.,
613 Peterson, L. C. and Toggweiler, J. R.: On the structure and origin of major glaciation cycles 1.
614 Linear responses to Milankovith forcing, Paleoceanography, 7(6), 701–738, 1992.

615 Jackson, M., Tyler, S., Willis, A., Bourbeau, G. and Pennington, R.: Weathering sequence of
616 clay-size minerals in soils and sediments. I. Fundamental Generalizations, J. Phys. Colloid
617 Chem., 52(7), 1237–1260 [online] Available from:
618 http://pubs.acs.org/doi/abs/10.1021/j150463a015 (Accessed 13 February 2015), 1948.

619 Jenny, H.: Factors of Soil Formation: A System of Quantitative Pedology, Dover Publications,
620 Inc, New York, New York. [online] Available from:
621 http://books.google.com/books?hl=en&lr=&id=orjZZS3H-
622 hAC&oi=fnd&pg=PP1&dq=Factors+of+Soil+Formation:+A+System+of+Quantitative+Pedolog
623 y&ots=fIfMb5fWkk&sig=e6Ev-CJjgsMYaO8DzFszbQK6Sss (Accessed 6 November 2014),
624 1941.

625 Jenny, H.: Derivation of state factor equations of soils and ecosystems, Soil Sci. Soc. Am. J.,
626 385–388 [online] Available from:
627 https://dl.sciencesocieties.org/publications/sssaj/abstracts/25/5/SS0250050385 (Accessed 29
628 January 2015), 1961.

629 Johnson, D. and Watson-Stegner, D.: Evolution model of pedogenesis, Soil Sci., 143(5), 349–
630 366 [online] Available from:
631 http://journals.lww.com/soilsci/Abstract/1987/05000/Evolution_Model_of_Pedogenesis.5.aspx
632 (Accessed 6 November 2014), 1987.

633 Lybrand, R. A. and Rasmussen, C.: Quantifying Climate and Landscape Position Controls on
634 Soil Development in Semiarid Ecosystems, Soil Sci. Soc. Am. J., 79(1), 104–116,
635 doi:10.2136/sssaj2014.06.0242, 2015.

636 Maejima, Y., Matsuzaki, H. and Higashi, T.: Application of cosmogenic 10Be to dating soils on
637 the raised coral reef terraces of Kikai Island, southwest Japan, Geoderma, 126(3-4), 389–399,
638 doi:10.1016/j.geoderma.2004.10.004, 2005.

639 McFadden, L. and Weldon, R.: Rates and processes of soil development on Quaternary terraces
640 in Cajon Pass, California, Geol. Soc. Am. Bull., 98, 280–293 [online] Available from:
641 http://gsabulletin.gsapubs.org/content/98/3/280.short (Accessed 28 May 2014), 1987.

642 McFadden, L., Wells, S. and Jercinovich, M.: Influences of eolian and pedogenic processes on
643 the origin and evolution of desert pavements, Geology, 15(June), 504–508 [online] Available
644 from: http://geology.gsapubs.org/content/15/6/504.short (Accessed 30 May 2015), 1987.

645 Merritts, D., Chadwick, O. and Hendricks, D.: Rates and processes of soil evolution on uplifted
646 marine terraces, northern California, Geoderma, 51, 241–275 [online] Available from:
647 http://www.sciencedirect.com/science/article/pii/0016706191900733 (Accessed 5 February
648 2015), 1991.

649 Minasny, B. and McBratney, A.: A rudimentary mechanistic model for soil production and
650 landscape development, Geoderma, 90, 3–21 [online] Available from:
651 http://www.sciencedirect.com/science/article/pii/S0016706198001153 (Accessed 6 November
652 2014), 1999.

653 Minasny, B. and McBratney, A.: A rudimentary mechanistic model for soil formation and
654 landscape development II. A two-dimensional model incorporating chemical weathering,
655 Geoderma, 103, 161–179 [online] Available from:
656 http://www.sciencedirect.com/science/article/pii/S0016706101000751 (Accessed 13 February
657 2015), 2001.

658 Muhs, D. R.: Intrinsic thresholds in soil systems., Phys. Geogr., 5, 99–110,
659 doi:10.1080/02723646.1984.10642246, 1984.

660 Muhs, D. R.: Evolution of Soils on Quaternary Reef Terraces of Barbados, West Indies, Quat.
661 Res., 56(1), 66–78, doi:10.1006/qres.2001.2237, 2001.

662 Muhs, D. R., Crittenden, R. C., Rosholt, J. N., Bush, C. A. and Stewart, K.: Genesis of marine
663 terrace soils, Barbados, West Indies: evidence from mineralogy and geochemistry., Earth Surf.
664 Process. Landforms, 12, 605–618, 1987.

665 Muhs, D. R., Bettis, E. a., Been, J. and McGeehin, J. P.: Impact of Climate and Parent Material
666 on Chemical Weathering in Loess-derived Soils of the Mississippi River Valley, Soil Sci. Soc.
667 Am. J., 65(6), 1761, doi:10.2136/sssaj2001.1761, 2001.

668 New, M., Hulme, M. and Jones, P.: Representing Twentieth-Century Space – Time Climate
669 Variability. Part I: Development of a 1961 – 90 Mean Monthly Terrestrial Climatology, J. Clim.,
670 12, 829–856 [online] Available from: http://journals.ametsoc.org/doi/full/10.1175/1520-
671 0442(1999)012%3C0829:RTCSTC%3E2.0.CO;2 (Accessed 21 July 2015), 1999.

672 Parsons, R. and Herriman, R.: A Lithosequence in the Mountains of Southwestern Oregon, Soil
673 Sci. Soc. Am. J., 39, 943–948 [online] Available from:
674 https://dl.sciencesocieties.org/publications/sssaj/abstracts/39/5/SS0390050943 (Accessed 13
675 February 2015), 1975.

676 Pelletier, J. D. and Rasmussen, C.: Geomorphically based predictive mapping of soil thickness in
677 upland watersheds, Water Resour. Res., 45(9), n/a–n/a, doi:10.1029/2008WR007319, 2009a.

678 Pelletier, J. D. and Rasmussen, C.: Quantifying the climatic and tectonic controls on hillslope
679 steepness and erosion rate, Lithosphere, 1(2), 73–80, doi:10.1130/L3.1, 2009b.

680 Petit, J., Jouzel, J., Raynaud, D. and Barkov, N.: Climate and atmospheric history of the past
681 420,000 years from the Vostok ice core, Antarctica, Nature, 399, 429–436 [online] Available
682 from: http://www.nature.com/articles/20859 (Accessed 15 February 2015), 1999.

683 Phillips, J. D.: An evaluation of the state factor model of soil ecosystems, Ecol. Modell., 45,
684 165–177 [online] Available from:
685 http://www.sciencedirect.com/science/article/pii/030438008990080X (Accessed 26 December
686 2014), 1989.

687 Phillips, J. D.: Progressive and Regressive Pedogenesis and Complex Soil Evolution, Quat. Res.,
688 40, 169–176 [online] Available from:
689 http://www.sciencedirect.com/science/article/pii/S0033589483710690 (Accessed 6 November
690 2014a), 1993.

691 Phillips, J. D.: Stability implications of the state factor model of soils as a nonlinear dynamical
692 system, Geoderma, 58(1-2), 1–15, doi:10.1016/0016-7061(93)90082-V, 1993b.

693 Portenga, E. W. and Bierman, P. R.: Understanding earth's eroding surface with 10Be, GSA
694 Today, 21(8), 4–10, doi:10.1130/G111A.1, 2011.

695 Pye, K.: Formation of quartz silt during humid tropical weathering of dune sands, Sediment.
696 Geol., 34, 267–282 [online] Available from:
697 http://www.sciencedirect.com/science/article/pii/0037073883900507 (Accessed 30 May 2015),
698 1983.

699 Pye, K. and Sperling, C. H. B.: Experimental investigation of silt formation by static breakage
700 processes: the effect of temperature, moisture and salt on quartz dune sand and granitic regolith,
701 Sedimentology, 30(1), 49–62, doi:10.1111/j.1365-3091.1983.tb00649.x, 1983.

Rasmussen, C.: Mass balance of carbon cycling and mineral weathering across a semiarid environmental gradient, Geochim. Cosmochim. Acta, 72(2008), A778, 2008.

Rasmussen, C. and Tabor, N. J.: Applying a Quantitative Pedogenic Energy Model across a Range of Environmental Gradients, Soil Sci. Soc. Am. J., 71(6), 1719, doi:10.2136/sssaj2007.0051, 2007.

Rasmussen, C., Southard, R. J. and Horwath, W. R.: Modeling Energy Inputs to Predict Pedogenic Environments Using Regional Environmental Databases, Soil Sci. Soc. Am. J., 69(4), 1266–1274, doi:10.2136/sssaj2003.0283, 2005.

Rasmussen, C., Troch, P. A., Chorover, J., Brooks, P., Pelletier, J. and Huxman, T. E.: An open system framework for integrating critical zone structure and function, Biogeochemistry, 102(1-3), 15–29, doi:10.1007/s10533-010-9476-8, 2011.

Rasmussen, C., Pelletier, J. D., Troch, P. A., Swetnam, T. L. and Chorover, J.: Quantifying Topographic and Vegetation Effects on the Transfer of Energy and Mass to the Critical Zone, Vadose Zo. J., doi:10.2136/vzj2014.07.0102, 2015.

Riebe, C. S., Kirchner, J. W. and Finkel, R. C.: Erosional and climatic effects on long-term chemical weathering rates in granitic landscapes spanning diverse climate regimes, Earth Planet. Sci. Lett., 224(3-4), 547–562, doi:10.1016/j.epsl.2004.05.019, 2004.

Runge, E. C. A.: Soil Development Sequences and Energy Models, Soil Sci., 115(3), 183–193, doi:10.1097/00010694-197303000-00003, 1973.

Salvador-Blanes, S., Minasny, B. and McBratney, a. B.: Modelling long-term in situ soil profile evolution: application to the genesis of soil profiles containing stone layers, Eur. J. Soil Sci., 58(6), 1535–1548, doi:10.1111/j.1365-2389.2007.00961.x, 2007.

Schaetzl, R. and Anderson, S.: Soils: Genesis and Geomorphology, First., Cambridge University Press, Cambridge, UK., 2005.

Sharmeen, S. and Willgoose, G.: The interaction between armouring and particle weathering for eroding landscapes, Earth Surf. Process. Landforms, 31, 1195–1210, doi:10.1002/esp, 2006.

Shoeneberger, P., Wysocki, D., Benham, E. and Soil Survey Staff: Field book for describing and sampling soils, Version 3., Natural Resources Conservation Service, National Soil Survey Center, Lincoln, NE. [online] Available from: http://scholar.google.com/scholar?hl=en&btnG=Search&q=intitle:Field+Book+for+Describing+and+Sampling+Soils#2 (Accessed 24 June 2015), 2012.

Smeck, N., Runge, E. and Mackintosh, E.: Dynamics and genetic modelling of soil systems, in Pedogenesis and Soil Taxonomy I. Concepts and Interactions, edited by L. Wilding, N. Smeck, and G. Hall, pp. 51–81, Elsevier, Amsterdam, ND., 1983.

736 Soil Survery Staff: Keys to Soil Taxonomy, 11th ed., United States Department of Agriculture,
737 National Resources Conservation Service., 2010.

738 Temme, A. J. A. M. and Vanwalleghem, T.: LORICA – A new model for linking landscape and
739 soil profile evolution: Development and sensitivity analysis, Comput. Geosci.,
740 doi:10.1016/j.cageo.2015.08.004, 2015.

741 Ugarte, M., Militino, A. and Arnholt, A.: Probability and Statistics with R, CRC Press, Boca
742 Raton, FL., 2008.

743 Vanwalleghem, T., Stockmann, U., Minasny, B. and McBratney, A. B.: A quantitative model for
744 integrating landscape evolution and soil formation, J. Geophys. Res. Earth Surf., 118(2), 331–
745 347, doi:10.1029/2011JF002296, 2013.

746 Volobuyev, V.: Ecology of soils, Academy of Sciences of the Azerbaijan SSR. Institute of Soil
747 Science and Agronomy. Israel Program for Scientific Translations., Jerusalem, Israel., 1964.

748 Wallace, J. M. and Hobbs, P. V: Atmospheric Science: An Introductory Survey, Second.,
749 Academic Press Inc., Amsterdam, ND., 2006.

750 West, N., Kirby, E., Bierman, P., Slingerland, R., Ma, L., Rood, D. and Brantley, S.: Regolith
751 production and transport at the Susquehanna Shale Hills Critical Zone Observatory, part 2:
752 Insights from meteoric10Be, J. Geophys. Res. Earth Surf., 118(3), 1877–1896,
753 doi:10.1002/jgrf.20121, 2013.

754 White, A. F., Bullen, T. D., Schulz, M. S., Blum, A. E., Huntington, T. G. and Peters, N. E.:
755 Differential rates of feldspar weathering in granitic regoliths, Geochim. Cosmochim. Acta, 65(6),
756 847–869, doi:10.1016/S0016-7037(00)00577-9, 2001.

757 Wilson, M. J.: Weathering of the primary rock-forming minerals: processes, products and rates,
758 Clay Miner., 39(3), 233–266, doi:10.1180/0009855043930133, 2004.

759 Yaalon, D.: Conceptual models in pedogenesis: Can soil-forming functions be solved?,
760 Geoderma, 14, 189–205 [online] Available from:
761 http://www.sciencedirect.com/science/article/pii/0016706175900014 (Accessed 14 February
762 2015), 1975.

763 Yoo, K. and Mudd, S. M.: Discrepancy between mineral residence time and soil age:
764 Implications for the interpretation of chemical weathering rates, Geology, 36(1), 35–38,
765 doi:10.1130/G24285A.1, 2008a.

766 Yoo, K. and Mudd, S. M.: Toward process-based modeling of geochemical soil formation across
767 diverse landforms: A new mathematical framework, Geoderma, 146(1-2), 248–260,
768 doi:10.1016/j.geoderma.2008.05.029, 2008b.

769 Yoo, K., Amundson, R., Heimsath, A. M., Dietrich, W. E. and Brimhall, G. H.: Integration of
770 geochemical mass balance with sediment transport to calculate rates of soil chemical weathering
771 and transport on hillslopes, J. Geophys. Res. F Earth Surf., 112(2), F02013,
772 doi:10.1029/2005JF000402, 2007.

773 Zachos, J., Pagani, M., Sloan, L., Thomas, E. and Billups, K.: Trends, rhythms, and aberrations
774 in global climate 65 Ma to present, Science (80-.)., 292(April), 686–694 [online] Available
775 from: http://www.sciencemag.org/content/292/5517/686.short (Accessed 14 February 2015),
776 2001.

777

SOIL Discuss., doi:10.5194/soil-2016-63, 2016
Manuscript under review for journal SOIL
Published: 18 October 2016

List of Figures and Tables

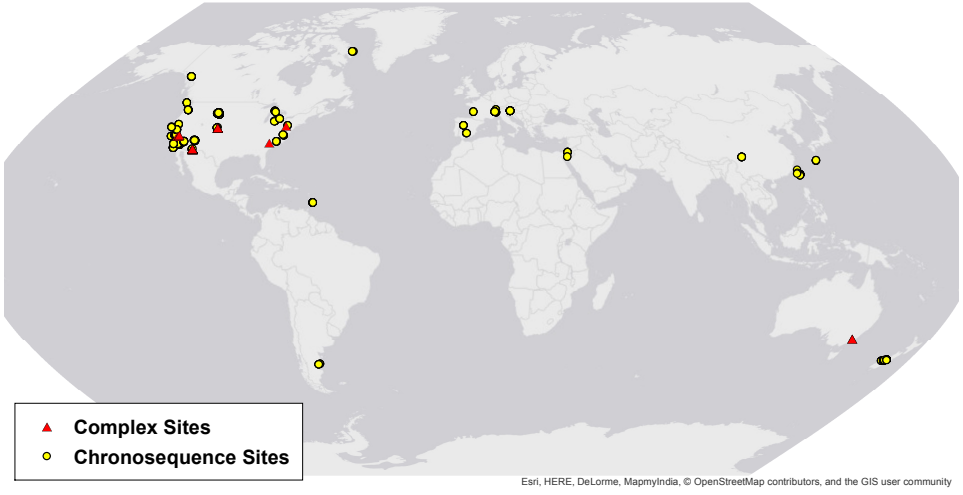

Figure 1. Map of study sites. Yellow points indicate location of chronosequences, and red triangles indicate location of soils in complex terrain.

SOIL Discuss., doi:10.5194/soil-2016-63, 2016
Manuscript under review for journal SOIL
Published: 18 October 2016

Table 1. Complex terrain study sites and characteristics.

Table 1. Complex terrain study sites and characteristics

Site	Study	Number of Sites	Elevation (m)	MAP (cm)	MAT (°C)	Parent Material	Slope	Aspect	Vegetation
Marshall Gulch Granite Subcatchment, Arizona, USA	Holleran et al., 2015. *SOIL*. 1:47-64. Lybrand and Rasmussen. 2015. *SSSAJ*. 79, 1: 104-116	24	2300-2500	85-90	10	Granite, Amphibolite, Quartzite	45%	North	*Pinus ponderosa, Pseudotsuga menziesii, Abies concolor*
Frog's Hollow, New South Wales, Australia	Yoo et al., 2007. *JGR*. 112: F02013	2	930	55-75	~16	Granodiorite	-	-	*Ecalyptus* grassland savannah
Cross Keys, South Carolina, USA	Bacon et al., 2012. *Geology*. 40, 9: 847-850	1	-	115-140	14-18	Granitic gneiss	<2%	-	*Quercus, Carya*
Gordon Gulch, Colorado, USA	Foster et al., 2015. *GSA Bulletin*. 127, 5/6: 862-878; Dethier et al., 2012. *Geomorph*. 173-174: 17-29	9	2440-2740	52	5	Gneiss, Quartz monzonite, granodiorite	15° - 28°	North and South	*Pinus ponderosa, Pinus contorta*
Rincon Mountains, Arizona, USA	Rasmussen, 2008. *Geochem. Cosmochem. Acta*. 72: A778.	11	1050-2500	<40-80	10-18	Granodiorite(?)	-	-	Oak grass woodland, Piñon-Juniper woodland, Mixed Conifer
Jemez Mountains, New Mexico, USA	Huckle et al., 2016. *Chem. Geol. in press.*	4	2990-3100	~50	4	Rhyolite, tuff	-	West and East	*Pseudotsuga menziesii, Abies concolor, Picea pungens, Populus tremuloides*
Shale Hills, Pennsylvania, USA	West et al., 2013. *JGR: Earth Surf*. 118: 1877-1896; Ma et al., unpublished	6	260-280	100	-	Shale, sandstone	15° - 20°	North and South	-
Sierra Nevada Mountains, California, USA	Dixon et al., 2009. *Earth Surf. Proc. Landf*. 34: 1507-1521	5	216-2991	37-106	3.9-16.6	Tonalite, granodiorite	-	-	Oak-grass woodland, Mixed Conifer, Subalpine

SOIL Discuss., doi:10.5194/soil-2016-63, 2016
Manuscript under review for journal SOIL
Published: 18 October 2016

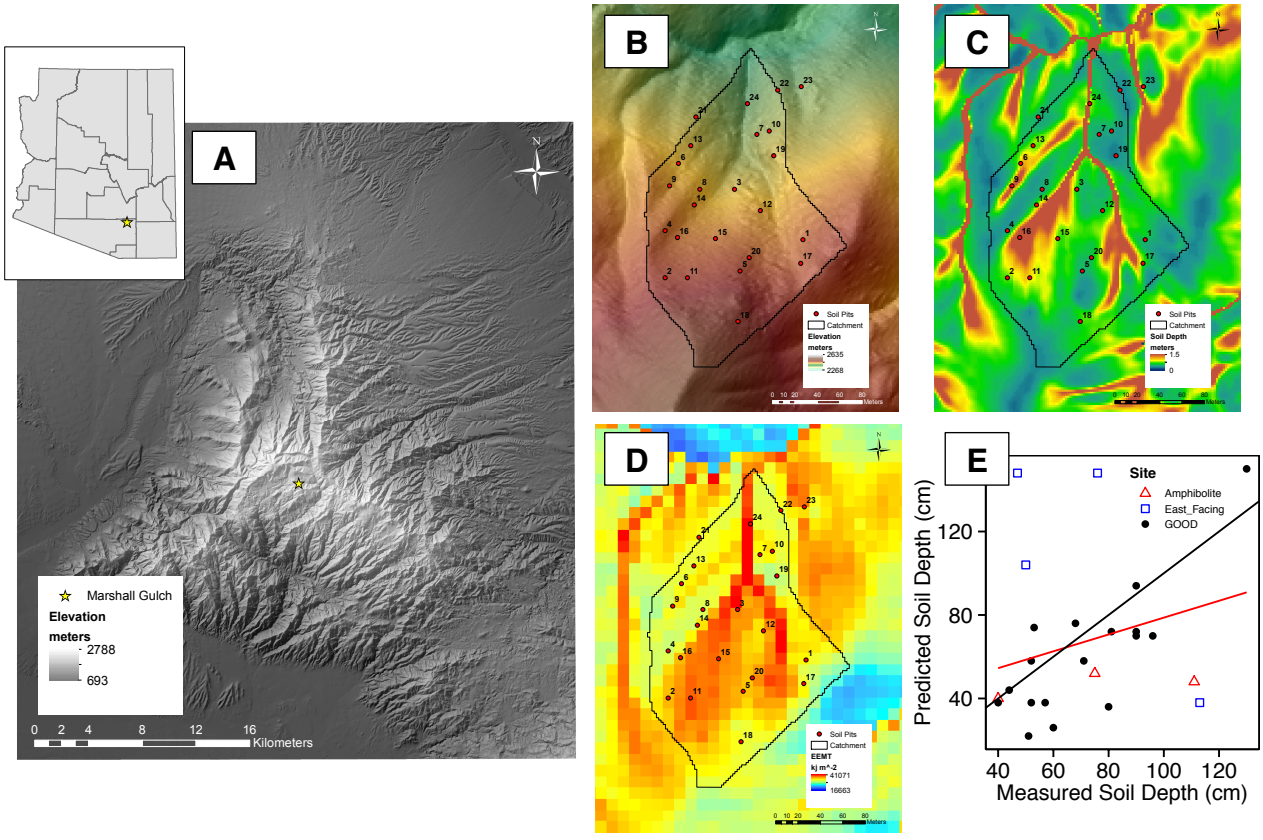

Figure 2. Marshall Gulch study site. (A) Location of the Santa Catalina Mountains and the Marshall Gulch catchment within Arizona, USA; (B) Elevation of the granite sub-catchment of Marshall Gulch; (C) Predicted soil depth in the granite sub-catchment (Pelletier and Rasmussen, 2009a); (D) EEMTv2.0 in the granite sub-catchment (Rasmussen et al., 2015); (E) Mismatch between the measured soil depths and predicted soil depths.

SOIL Discuss., doi:10.5194/soil-2016-63, 2016
Manuscript under review for journal SOIL
Published: 18 October 2016

Table 2. Parameters for the bivariate normal probability distributions for the soil physical properties and TPE.

Table 2. Soil property parameters

Variable	n	μ	σ	ρ[a]
Max Sand	398	70.51	25.39	-0.48
Max Silt	398	34.80	18.38	0.32
Max Clay[b]	416	4.52	2.24	0.78
DWT Sand	398	59.03	26.04	-0.57
DWT Silt[b]	398	4.55	1.68	0.26
DWT Clay[b]	416	3.66	2.09	0.73
Solum Thickness[c]	410	1.77	0.52	0.65
TPE[c]	416[d]	8.71	1.29	-
	398[e]	8.72	1.28	-
	410[f]	8.73	1.26	-

[a]ρ, Pearson correlation between soil variables and Total Pedogenic Energy

[b]Square root transformed

[c]Log10 transformed

[d]For clay variables

[e]For sand and silt variables

[f]For solum thickness

n = number of profiles, μ = mean, σ = standard deviation

Max indicates maximum content

DWT indicates depth weighted average content

SOIL Discuss., doi:10.5194/soil-2016-63, 2016
Manuscript under review for journal SOIL
Published: 18 October 2016

Table 3. Spearman rank correlations between soil physical properties and TPE and age.

Table 3. Spearman Rank Correlations

Variable	NPP	MAP	MAT	TPE	Age	% Increase[a]	n
Max Sand	-0.30	-0.10	-0.26	-0.46	-0.37	22.4	398
Max Silt	-0.03	-0.16	0.09	0.31	0.32	-4.5	398
Max Clay	0.15	-0.01	0.36	0.80	0.73	9.3	416
DWT Sand	-0.22	-0.04	-0.29	-0.57	-0.50	14.1	398
DWT Silt	0.05	-0.06	0.06	0.24	0.23	1.9	398
DWT Clay	0.21	0.02	0.39	0.75	0.67	12.4	416
Solum Thickness	0.12	0.06	0.22	0.63	0.57	10.4	410

Max indicates maximum content
DWT indicates depth weighted average content
[a]Precent increase in Spearman rank correlation between TPE and age

SOIL Discuss., doi:10.5194/soil-2016-63, 2016
Manuscript under review for journal SOIL
Published: 18 October 2016

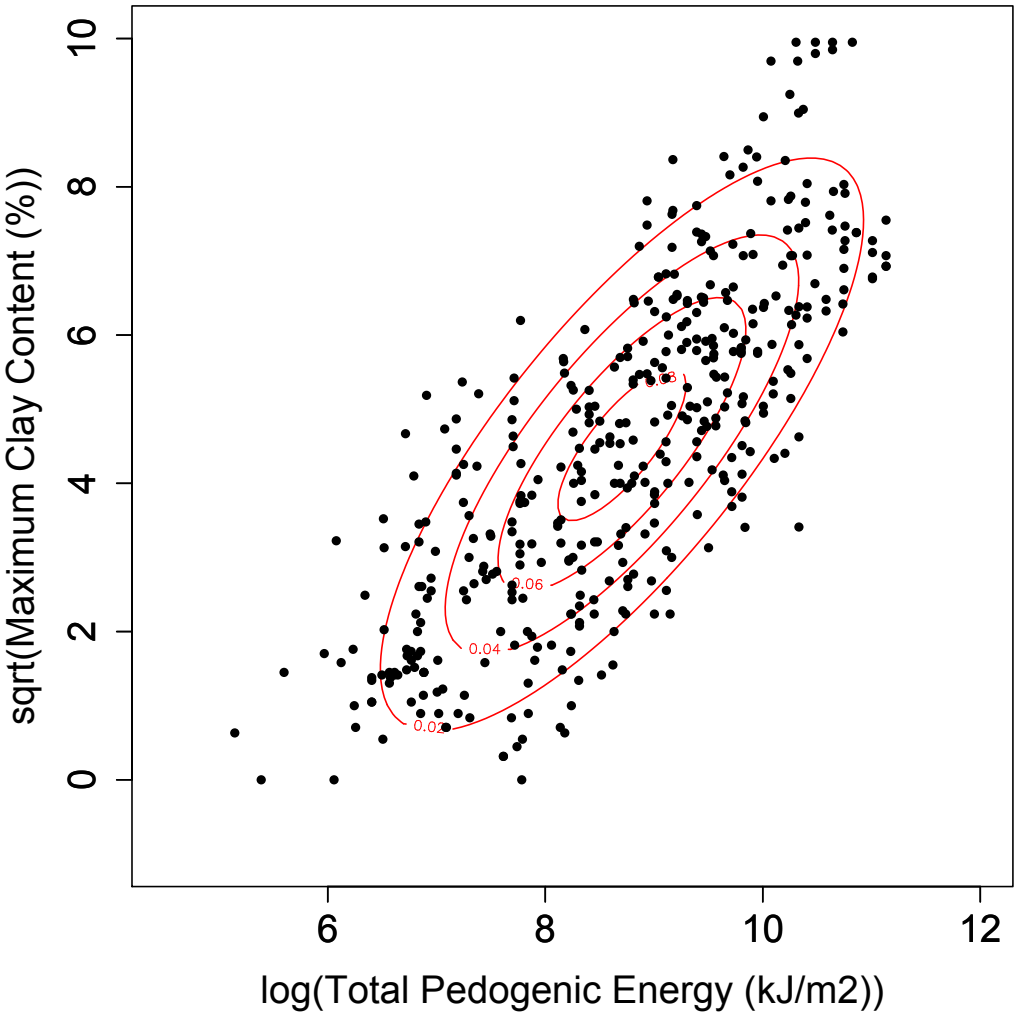

Figure 3. Bivariate normal distribution between TPE and max clay content. The points indicate individual soils. The red ellipses represent lines of equal probability, which corresponds to a three dimensional probability distribution. From this relationship the conditional mean and variances for the soil physical properties were calculated.

SOIL Discuss., doi:10.5194/soil-2016-63, 2016
Manuscript under review for journal SOIL
Published: 18 October 2016

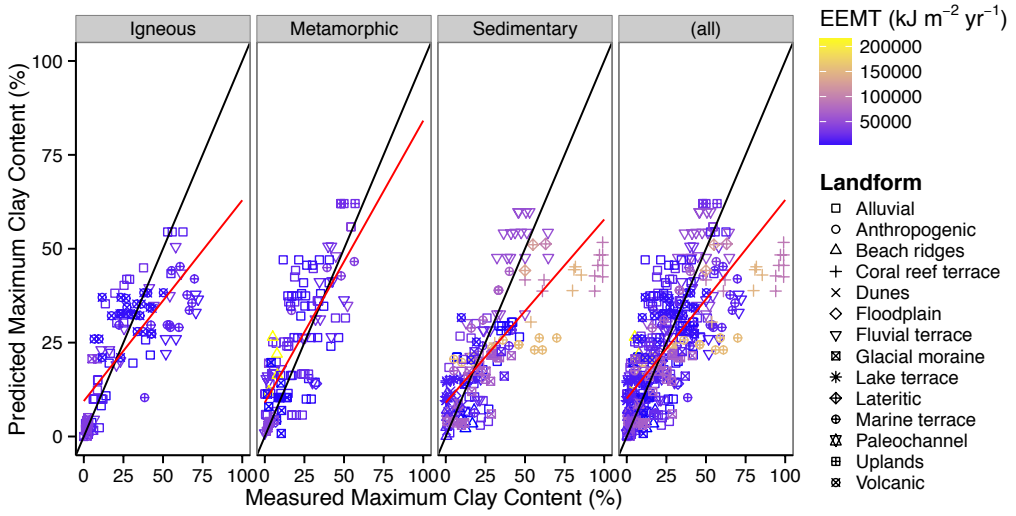

Figure 4. LOOCV results for max clay content. The results were subdivided by general soil parent material: igneous, metamorphic, and sedimentary; the points represent the geomorphic surface each soil formed on, and the colors represents the EEMT value for the location of each soil. Using LOOCV, where one chronosequence was removed from the model dataset and the remaining datasets were used to predict the parameters of the bivariate distributions, the conditional means of the left out chronosequence was determined. The model was effectively able to predict the conditional mean values of the max clay contents with an r^2=0.54 (RMSE=14.7%). The model was least capable of predicting the clay contents on coral reef terraces (+), and appeared the most effective for alluvial surfaces (□).

SOIL Discuss., doi:10.5194/soil-2016-63, 2016
Manuscript under review for journal SOIL
Published: 18 October 2016

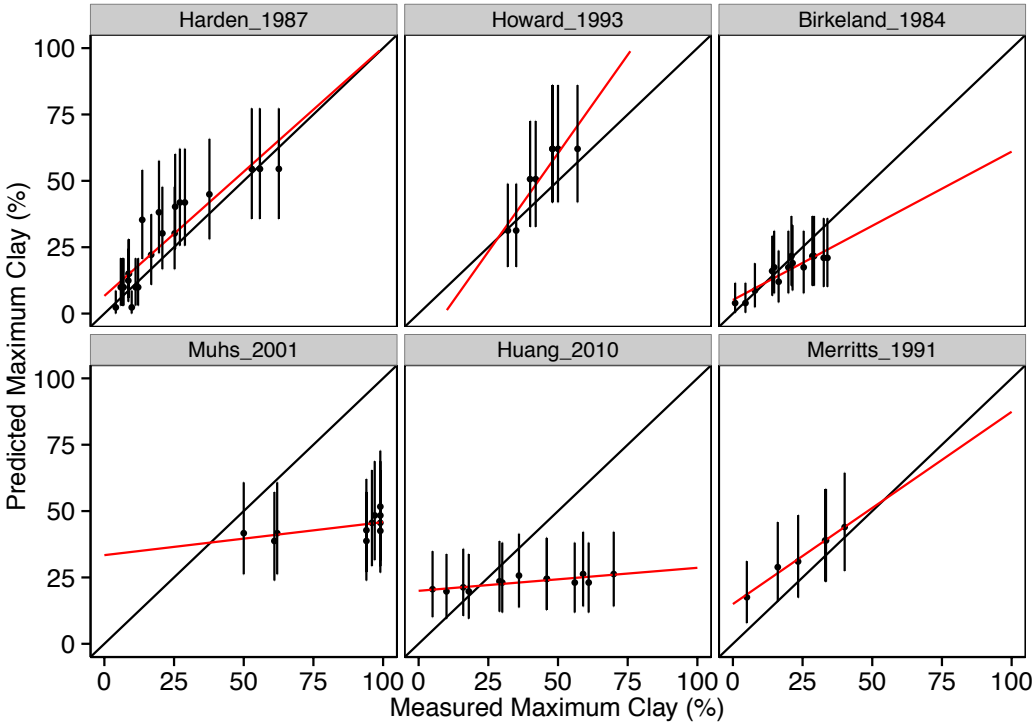

Figure 5. Selected relationships between the measured maximum clay content and predicted maximum clay content. A) Harden, 1987, B) Howard et al., 1993, C) Birkeland 1984, D) Muhs, 2001, E) Huang et al., 2010, and F) Merritts et al., 1991. The errors represent the conditional standard deviations around the mean, which correspond to a probability of 50%. The model effectively predicted clay content across a diverse range of climates, landforms, and parent materials. The model was the least effective at predicting the clay content of soils in tropical climates, and soils forming on coral reef terraces.

SOIL Discuss., doi:10.5194/soil-2016-63, 2016
Manuscript under review for journal SOIL
Published: 18 October 2016

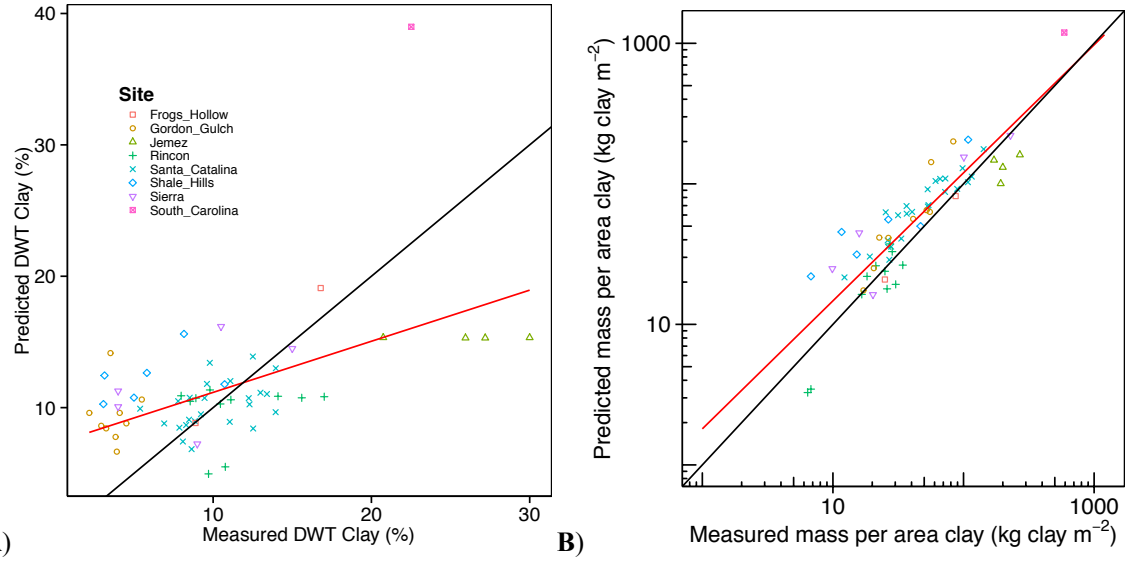

Figure 6. Model results in complex terrain. (A) Prediction of depth weighted (DWT) clay contents; (B) Prediction of mass per area clay using Eq. 9. The model was incapable of directly predicting DWT clay for the soils in complex terrain due to redistributive hillslope processes, r^2=0.25 between measured and predicted conditional mean DWT clay (A). By including information about soil depth and percent volume rock fragment, and converting DWT clay to mass per area clay, the model was significantly more effective at predicting clay contents for these soils r^2=0.81.

SOIL Discuss., doi:10.5194/soil-2016-63, 2016
Manuscript under review for journal SOIL
Published: 18 October 2016

Table 4. Sensitivity analysis of model prediction in complex terrain.

Table 4. Sensitivity analysis of model prediction in complex terrain

Effects	DF	Sums of Squares	Mean Sums of Squares	F value	p
Depth, h (cm)	1	1129156	1129156	469.0	< 2e-16
CM DWT Clay, $\mu_{Y|X=x}$ (%)	1	142430	142430	59.2	2.0E-10
Rock fragment, RF% (%)	1	3013	3013	1.3	0.27
Residuals	58	139632	2407		

SOIL Discuss., doi:10.5194/soil-2016-63, 2016
Manuscript under review for journal SOIL
Published: 18 October 2016

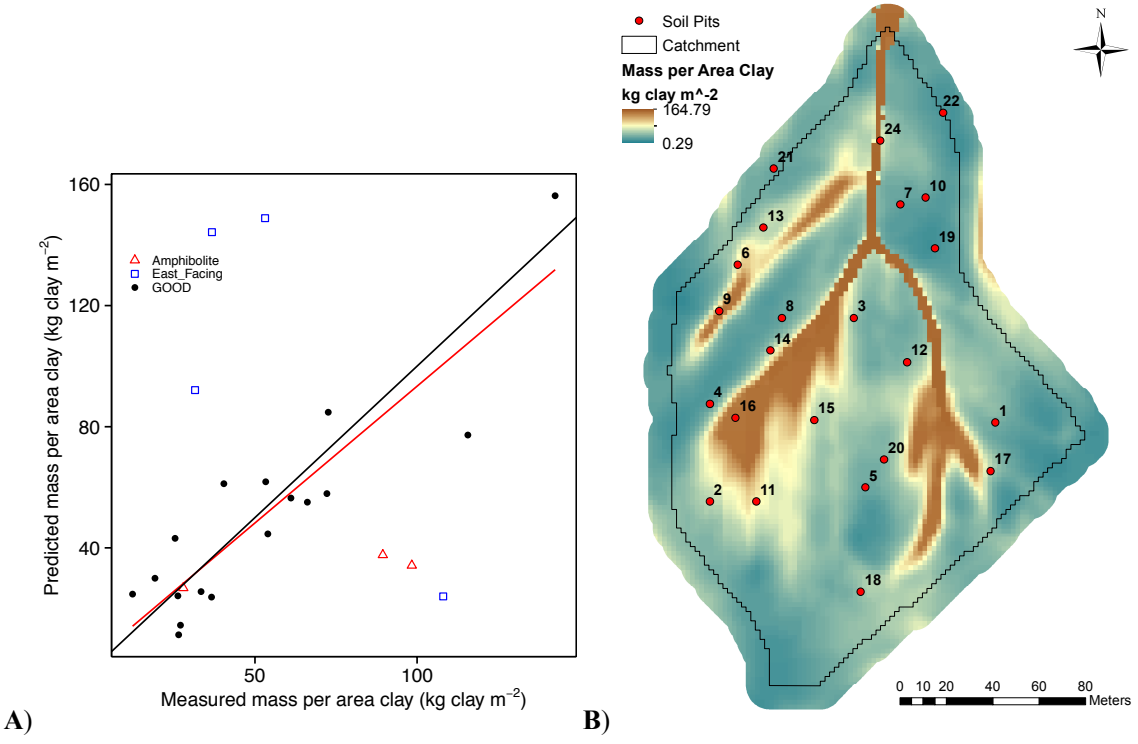

Figure 7. Model results of coupled geomorphic-EEMT-TPE model in Marshall Gulch granite sub-catchment. (A) Prediction of mass per area clay for sites from Holleran et al. (2015) and Lybrand and Rasmussen et al. (2015); (B) Spatial prediction of mass per area clay When combining the present approach, with a geomorphic based soil depth model, the combined models together were highly effective at predicting the clay contents for a majority of soils in the Santa Catalina Mountains (Catalina-Jemez CZO), r^2=0.74.